Measurements of the reaction $\bar{p}p \rightarrow \phi\eta$ of antiproton annihilation at rest at three hydrogen target densities

The OBELIX Collaboration.

Abstract

The $\bar{p}p$ annihilation at rest into the $\phi\eta$ final state was measured for three different target densities: liquid hydrogen, gaseous hydrogen at NTP and at a low pressure of 5 mbar. The yield of this reaction in the liquid hydrogen target is smaller than in the low-pressure gas target. The branching ratios of the $\phi\eta$ channel were calculated on the basis of simultaneous analysis of the three data samples. The branching ratio for annihilation into $\phi\eta$ from the $^3S_1$ protonium state turns out to be about ten times smaller as compared to the one from the $^1P_1$ state.

The Okubo-Zweig-Iizuka (OZI) rule [1] allows one to relate the ratio between the cross sections or annihilation frequencies of ϕ and ω meson production to the mixing angle Θ of the vector meson nonet:

$$R = \frac{\mathcal{F}(\bar{p}+p \to \phi + X)}{\mathcal{F}(\bar{p}+p \to \omega + X)} = tan^2\delta \cdot f = 4.2 \cdot 10^{-3} \cdot f \quad (1)$$

Here $\delta = \Theta - \Theta_0$, where $\Theta = 39^0$ from the quadratic Gell-Mann-Okubo mass formula, $\Theta_0 = 35.3^0$ is the ideal mixing angle and f is a kinematic phase space factor. It is known that the predictions of the OZI rule are fulfilled in the hadronic interactions at a level of about 10% (for a review, see [2]). Recently large OZI rule violation has been found in some $\bar{p}p$ annihilation channels in the experiments with stopped antiprotons at LEAR (CERN). Measurements of the Crystal Barrel collaboration show that the ratio of yields for the reactions $\bar{p}+p \to \phi(\omega)+\gamma$ is $R(\phi\gamma/\omega\gamma) = (250 \pm 89) \cdot 10^{-3}$ [3]. Large apparent violation of the OZI rule was also found for the $\bar{p}+p \to \phi(\omega)+\pi^0$ channel, where $R(\phi\pi^0/\omega\pi^0) = (96 \pm 15) \cdot 10^{-3}$ for annihilation in the liquid hydrogen target [3] and $R(\phi\pi^0/\omega\pi^0) = (114 \pm 24) \cdot 10^{-3}$ for annihilation in the gas hydrogen target [4]. Conservation of P- and C-parities allows the $\bar{p}p \to \phi\pi$ reaction only from the $^3S_1$ or $^1P_1$ initial states. An interesting dynamical selection rule was found for this channel: ϕ production is at least 15 times more prominent for annihilation from the spin triplet $^3S_1$ initial state than from the singlet $^1P_1$ one [5].

On the other hand, there are channels of ϕ meson production in $\bar{p}p$ annihilation at rest where no OZI rule violation was observed. An example is the reaction

$$\bar{p}+p \quad \longrightarrow \quad \phi+\eta, \quad (2)$$

where the Crystal Barrel collaboration found [6],[3] that the ratio R for annihilation in liquid $R(\phi\eta/\omega\eta) = (6.0 \pm 2.0) \cdot 10^{-3}$ is in agreement with the OZI rule prediction [1]. Since reaction (2) proceeds from the same protonium levels as the $\bar{p}p \to \phi\pi^0$ reaction, but from isospin I=0, one may expect that the $\phi\eta$ final state will also be suppressed for annihilation from the $^1P_1$ state. Surprisingly enough, the result reported here shows that the situation is opposite: the yield of reaction (2) for annihilation from the P-wave is higher than from the S-wave.

We performed systematic measurements of the channel

$$\bar{p}+p \quad \longrightarrow \quad K^+ + K^- + \eta \quad (3)$$

at rest in a hydrogen target of three densities: liquid, gaseous at NTP and at 5 mbar. Changing the target pressure allowed selection of the $\bar{p}p$ initial state. The fraction of annihilation from the S-wave decreases with decreasing target density. According to [7], it varies from 87% to 20% for annihilation in liquid and 5 mbar hydrogen, respectively.

Earlier we reported [4] measurements of reaction (2) for annihilation in a gas target at NTP, though with considerably lower statistics. The measurements of this reaction for the 5 mbar hydrogen target are made for the first time.

The experiment was performed at LEAR (CERN), using the OBELIX spectrometer [8]. The experimental setup consists of detectors arranged around the Open Axial Field Magnet, which provided the magnetic field of 0.5 T along the beam axis. The Time of Flight (TOF) system contains two coaxial barrels of plastic scintillators for charged particle identification and the trigger. The Jet Drift Chamber (JDC) provides tracking and particle identification by energy loss measurement. The High Angular Resolution Gamma Detector (HARGD) is designed to detect neutral particles by their decay into γ. Only the information of the TOF and JDC systems was used in the present analysis. All data were collected with the trigger requesting two hits in the inner barrel of scintillators and two hits in the outer one.

Two-prong events with the total charge zero and with the length of both tracks more than 20 cm for each data sample were selected. Kaons were identified by dE/dx measurements. We required both particles to be identified as kaons. The number of events in the data samples, the number of events that passed quality cuts, and particle identification N_{KKX} are presented in Table 1.

Table 1: Summary of the collected statistics. The number of events on the tape, which passed quality cuts (two-prong events with the total charge zero and with the length of both tracks more than 20 cm) and were identified as kaons are given.

Target	On tape ($\cdot 10^6$)	After quality cuts ($\cdot 10^6$)	N_{KKX} ($\cdot 10^5$)
Liquid	10.4	6.7	1.81
Gas at NTP	6.7	4.5	1.06
Gas at 5 mbar	9.4	5.4	1.71

The experimental distributions of the K^+K^-X final state for three data samples without correction for the acceptance are shown in Fig. 1 (left to right: liquid, gas at NTP and gas at 5 mbar). The scatter plots of missing mass squared distributions *vs* $M_{K^+K^-}$ are shown in Figs. 1a-c. One can see two horizontal bands from reactions with π^0 and η. The accumulation of events seen on the left side of the plots corresponds to the $\phi\pi^0$ final state. In the right corner of the plots there is a spot from $\bar{p}p \to K^+K^-$ reaction and an inclined band from the $\pi^+\pi^-X$ final state with wrongly identified pions. To see more clearly the region of these plots around the η band we zoomed them in the centre (Fig.1 d,e,f). A blob from the $\phi\eta$ events is better seen in these plots. Figures 1g,h,i show the distributions of the missing mass square recoiling against the two charged kaons, where the peaks due to reaction (3) are seen.

To select events from the $\phi\eta$ reaction the invariant mass distribution of two kaons $M_{K^+K^-}$ for events with the missing mass around the mass of η was analysed. It is shown in the middle part of Fig.2, where events with the missing mass interval $0.26 < M^2_{miss} < 0.34 \;\; GeV^2/c^4$ (centred around $m^2_\eta = 0.3 \;\; GeV^2/c^4$) were selected. The left and right parts of Fig.2 correspond to the $M_{K^+K^-}$ distributions for the missing mass intervals below and above the η mass, where number of events with η is negligible: $0.15 < M^2_{miss} < 0.23$ (left) and $0.37 < M^2_{miss} < 0.45 \;\; GeV^2/c^4$ (right). For the sake of brevity we label the missing mass intervals "A", "B" ,"C" in order of increasing M^2_{miss}.

To illustrate the choice of the intervals in Fig.3 the distributions on M^2_{miss} obtained by the Monte Carlo simulation of reaction (2) and the main background reactions are shown. One can see that the interval "B" contains most of the events from the reaction of interest. The background reaction

$$\bar{p} + p \quad \longrightarrow \quad \phi + \pi^0 + \pi^0 \tag{4}$$

gives the main contribution in interval "A" , whereas the events from the $\phi\pi^0\pi^0\pi^0$ final state concentrate mainly in the interval "C".

The experimental distributions for the interval "B" (Figs. 2b, 2e and 2h) for events with missing mass around the mass of η show clear peaks in the region of the ϕ meson. The ϕ signal for events from neighbouring missing mass intervals "A" and "C" is far less pronounced.

To describe the ϕ peak in $M_{K^+K^-}$ spectra we used the Breit-Wigner function, corrected for phase space, centrifugal factor and convoluted with a gaussian experimental resolution function. The background was treated by a smooth third-order polynomial function.

The ϕ peak positions are $1018 \pm 1 \;\; MeV/c^2, 1019 \pm 1 \;\; MeV/c^2$ and $1020 \pm 1 \;\; MeV/c^2$ for the LQ, NTP and 5 mbar data samples, respectively; these values agree well with the PDG value for the ϕ mass. The widths of the gaussian, which corresponds to the detector resolution, are $4.3 \pm 0.3 \;\; MeV/c^2, \;\; 3.4 \pm 0.3 \;\; MeV/c^2$ and $3.7 \pm 0.4 \;\; MeV/c^2$ for the LQ, NTP and 5 mbar data samples, respectively. They are in agreement with those obtained by the Monte Carlo simulation.

To evaluate contamination from the background reactions $\bar{p}p \to \phi X$ in missing mass interval "B", the number of events with ϕ mesons in neighbouring intervals "A" and "C" was determined. The background was subtracted assuming smooth behaviour of the squared missing mass distribution. Monte Carlo simulation of different background channels confirmed this assumption.

The main background contribution is from the reaction $\bar{p}p \to \phi\pi^0\pi^0$. Using the preliminary results for the frequency of this channel obtained by the Crystal Barrel collaboration with the liquid target $\mathcal{F}(\phi\pi^0\pi^0) = (0.88 \pm 0.15) \cdot 10^{-4}$ [9] one may estimate the number of $\phi\pi^0\pi^0$ events in

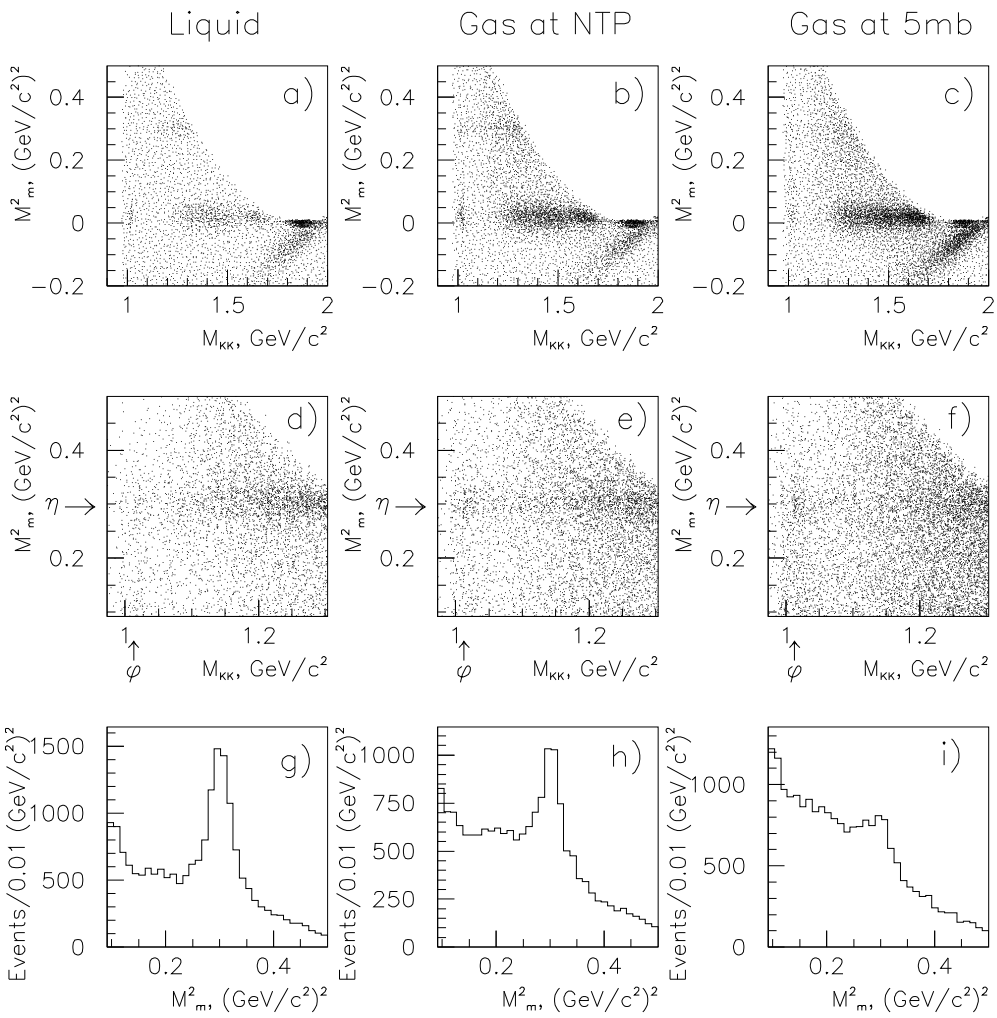

Figure 1: Scatter plots of missing masses *vs* $M_{K^+K^-}$ (a,b,c). The same distributions around the η band are shown in (d,e,f); missing mass spectra (g,h,i). The left column corresponds to the data at the liquid target, the middle one to the target at NTP and (c,f,i) to the target at 5 mbar.

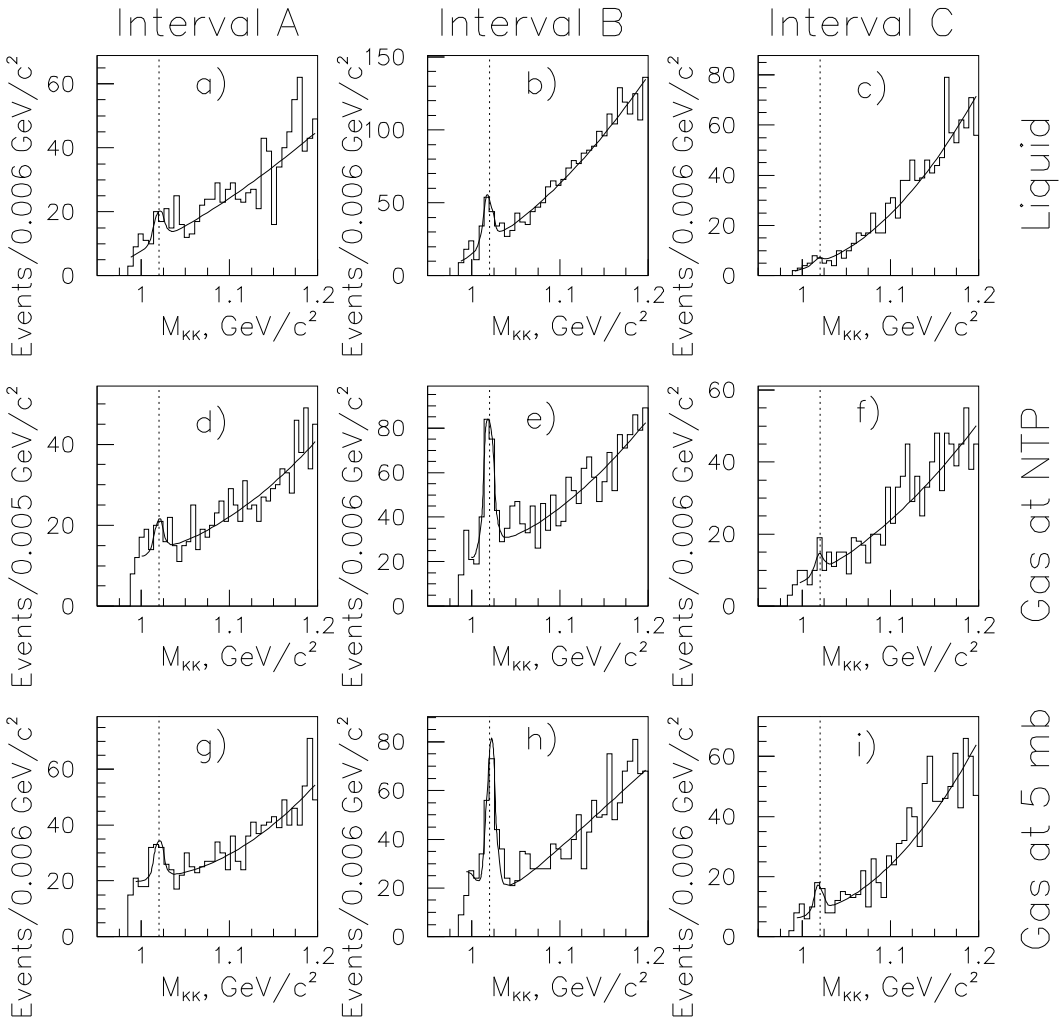

Figure 2: The distributions on $M_{K^+K^-}$ for three intervals of missing mass for three target densities: (a,b,c) for the liquid target, (d,e,f) for the gas target at NTP and (g,h,i) for the gas target at 5 mbar. The left column corresponds to interval "A" (see the text), column (b,e,h) corresponds to interval "B", and column (c,f,i) corresponds to interval "C". Dashed lines correspond to the ϕ meson mass.

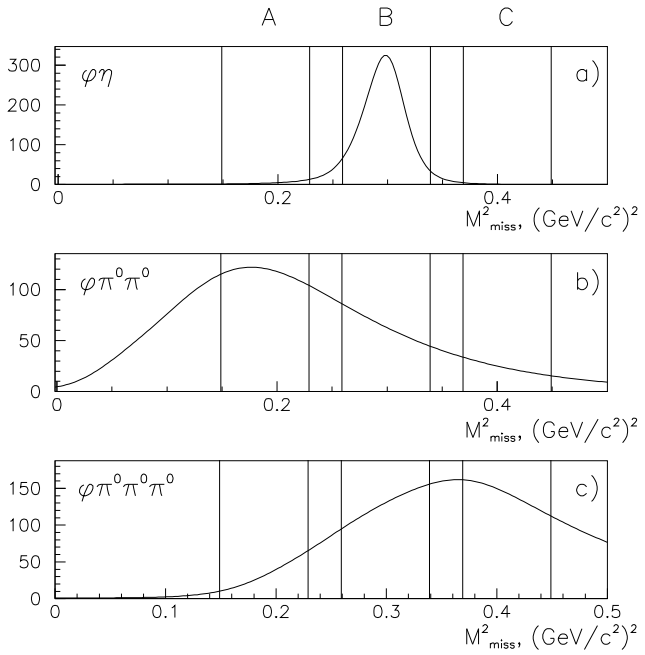

Figure 3: The spectra of missing mass recoiling against K^+K^- system for a) $\bar{p}p \to \phi\eta$ reaction, b) $\bar{p}p \to \phi\pi^0\pi^0$ and c) $\bar{p}p \to \phi\pi^0\pi^0\pi^0$, obtained by Monte Carlo. Lines show the interval limits.

interval "B": $N_{ev} = \mathcal{F} \cdot N_{ann} \cdot \varepsilon_{reg} = (0.88 \pm 0.15) \cdot 10^{-4} \cdot (115.9 \cdot 10^6) \cdot (0.165 \pm 0.010) \cdot 10^{-2} = 17 \pm 3$. It is in good agreement with our estimation of the background, which gives 17 ± 13 events.

We also verify the contamination from the channels $\bar{p}p \to \phi X$, where X decays into charged particles which are not registered by our apparatus. For this purpose, the registration efficiency was determined for the reaction $\bar{p}p \to \phi\rho$, when both pions from ρ decay were missed. It turns out to be $\varepsilon_{reg} = 1.0 \cdot 10^{-5}$. With the known frequency of $\bar{p}p \to \phi\rho$ in NTP $\mathcal{F} = (3.4 \pm 0.8) \cdot 10^{-4}$ [10], the estimated number of events from this reaction in interval "B" is $N_{ev} \approx 0.2 \pm 0.1$.

The annihilation frequency $\mathcal{F}$ is

$$\mathcal{F} = \frac{N_{ev}}{N_{ann} \cdot \varepsilon_{reg}} \tag{5}$$

where N_{ann} is the number of annihilations in the target and ε_{reg} is the registration efficiency that takes into account the correction for all ϕ and η decay modes.

The simulation of reaction (2) shows that the registration efficiency ε_{reg} for annihilation from the $^1P_1$ initial state is less than from the $^3S_1$ one. Without information about relative abundances of these initial states for annihilation in different targets one could determine only an upper and lower limits for the annihilation frequency, corresponding to the initial states $^1P_1$ and $^3S_1$, respectively.

In Table 2, the number of annihilations N_{ann}, the number of events from the reaction N_{ev}, the registration efficiency ε_{reg} and the upper and lower limits for the frequencies of the channel $\bar{p}p \to \phi\eta$ for each sample are presented.

The systematic uncertainties in the evaluation of the annihilation frequencies are about 8%. The systematics includes beam monitoring, trigger inefficiencies and the uncertainties due to varying the dE/dx kaon selection criteria.

It is possible to determine the branching ratios *B.R.* of the reaction $\bar{p}p \to \phi\eta$ by using additional information from some models of the protonium atoms. Let us divide the number of

Table 2: Number of annihilations N_{ann}, number of events N_{ev}, registration efficiency ε_{reg} and upper and lower limits of the annihilation frequencies $\mathcal{F}$ for each sample.

Target	$N_{ann} \cdot 10^6$	N_{ev}	$\varepsilon_{reg}, \%$	$\mathcal{F} \cdot 10^4$	Initial state
Liquid	115.9	68 ± 22	0.97 ± 0.02	0.60 ± 0.20	$^3S_1$
			0.58 ± 0.02	1.01 ± 0.33	$^1P_1$
Gas at NTP	74.5	146 ± 28	1.88 ± 0.03	1.04 ± 0.20	$^3S_1$
			1.28 ± 0.03	1.53 ± 0.29	$^1P_1$
Gas at 5 mbar	85.9	152 ± 37	1.68 ± 0.03	1.05 ± 0.26	$^3S_1$
			1.09 ± 0.03	1.62 ± 0.40	$^1P_1$

ϕ events N_{ev} in each data sample into two contributions

$$N_{ev} = N_{ev}(^3S_1) + N_{ev}(^1P_1) \tag{6}$$

which are defined, according to Batty [7], as

$$N_{ev}(^3S_1) = (1 - f_p) \cdot \frac{3}{4} \cdot E(^3S_1) \cdot B.R.(^3S_1) \cdot N_{ann} \cdot \varepsilon_{reg}(^3S_1) \tag{7}$$

$$N_{ev}(^1P_1) = f_p \cdot \frac{3}{12} \cdot E(^1P_1) \cdot B.R.(^1P_1) \cdot N_{ann} \cdot \varepsilon_{reg}(^1P_1) \tag{8}$$

Here f_p is the fraction of annihilations from the P-states, factors $\frac{3}{4}$ and $\frac{3}{12}$ are the statistical weights of the $^3S_1$ and $^1P_1$ states, respectively. $E(^3S_1)$ and $E(^1P_1)$ are the enhancement factors which reflect deviations from the pure statistical population of the level. The values of f_p and enhancement factors are taken from [7] and shown in Table 3.

The branching ratio B.R. is the probability that the $\bar{p}p$ system with the definite quantum numbers J^{PC} of the initial state annihilates into a given final state. Since our measurements at three hydrogen target densities give three values of N_{ev}, it is possible to determine the two unknown parameters $B.R.(^3S_1 \to \phi\eta)$ and $B.R.(^1P_1 \to \phi\eta)$ from eqs. (6)-(8).

By using the enhancement factors from [7] for the DR1 model and considering for the annihilation frequency of $\bar{p}p \to \pi^0\pi^0$ reaction in liquid the value of $(2.8 \pm 0.4) \cdot 10^{-4}$ [11], we obtain a different set of values for f_p shown in Table 3, which is useful for testing the stability of our results.

Table 3: Fraction of P-wave annihilation f_p taken from the analyses of [7] and [11] and the enhancement factors E from [7].

	f_p		Enhancement factors	
Target	[11]	[7]	$E(^3S_1)$	$E(^1P_1)$
Liquid	0.06 ± 0.01	0.13 ± 0.04	0.989	0.856
Gas at NTP	0.56 ± 0.04	0.58 ± 0.06	0.993	0.974
Gas at 5 mbar	0.84 ± 0.03	0.80 ± 0.06	0.985	0.999

The branching ratios obtained from the fit of the events at three densities are:

$$B.R.(^3S_1 \to \phi\eta) = (0.76 \pm 0.31) \cdot 10^{-4} \tag{9}$$

$$B.R.(^1P_1 \to \phi\eta) = (7.78 \pm 1.65) \cdot 10^{-4} \tag{10}$$

for the parameters choice [7] and

$$B.R.(^3S_1 \to \phi\eta) = (0.82 \pm 0.28) \cdot 10^{-4} \tag{11}$$

$$B.R.(^1P_1 \to \phi\eta) = (7.59 \pm 1.55) \cdot 10^{-4} \tag{12}$$

for the parameters from [11]. Therefore, for both sets of f_p the branching ratio of $\bar{p}p \to \phi\eta$ channel for annihilation from the spin singlet $^1P_1$ state is about 10 times higher than the branching ratio from the spin triplet $^3S_1$ state. An opposite trend was observed for the $\bar{p}p \to \phi\pi^0$ channel [5].

Using the branching ratios obtained above, the annihilation frequencies at different hydrogen target densities can be calculated:

$$\mathcal{F} \quad = \quad (1 - f_p) \cdot \frac{3}{4} \cdot E(^3S_1) \cdot B.R.(^3S_1) + f_p \cdot \frac{3}{12} \cdot E(^1P_1) \cdot B.R.(^1P_1). \tag{13}$$

The corresponding results are presented in Table 4.

Table 4: Annihilation frequencies $\mathcal{F} \cdot 10^4$ calculated from (13) with B.R. from (9)-(12). The upper numbers correspond to the P-wave fraction calculated with the parameters of [7] and the lower numbers correspond to the parameters of [11].

Reference	Liquid	Gas at NTP	Gas at 5 mbar
[7]	0.71 ± 0.07	1.33 ± 0.15	1.66 ± 0.20
[11]	0.67 ± 0.07	1.30 ± 0.14	1.69 ± 0.21

One could see that in spite of the significant difference in the branching ratios from the S- and P-wave states the annihilation frequencies increase only by a factor of two from the liquid to the 5 mbar sample. It is due to the relatively small statistical weight of the $^1P_1$ state.

Several experimental studies of the $\phi\eta$ antiproton annihilation channel at rest have been reported. The results of these measurements are shown in Table 5. The Crystal Barrel collaboration measured the $\bar{p}p \to \phi\eta$ channel for annihilation in liquid hydrogen [6]. The absolute value for the annihilation frequency was not determined but the ratio to the $\bar{p}p \to \phi\pi^0$ frequency was given. The value in Table 5 was deduced from this ratio and from the annihilation frequency of the $\bar{p}p \to \phi\pi^0$ channel measured by the same collaboration [3]. It is in good agreement with our result for annihilation in liquid shown in Table 2 and Table 4.

Table 5: Experimental results of the previous measurements of the $\bar{p}p \to \phi\eta$ channel at rest.

Reference	$\mathcal{F} \times 10^4$	Comments
[6], [3]	0.66 ± 0.19	liquid target
[12]	0.37 ± 0.09	gas at NTP
[12]	0.41 ± 0.16	gas at NTP, LX-trigger
[4]	$1.04 \pm 0.33 \pm 0.05$	gas at NTP, upper limit
[4]	$0.74 \pm 0.22 \pm 0.03$	gas at NTP, lower limit

The ASTERIX collaboration [12] measured the $\phi\eta$ channel for antiproton annihilation in a gas target at NTP. Beside it the yield of (2) was measured with the so-called LX-trigger, which enriched the data sample with P-wave annihilation events. Our results for the gas target at NTP shown in Table 2 and Table 4 disagree with the absolute values of the ASTERIX collaboration.

The previous measurements of the OBELIX collaboration [4], performed with a gas NTP target with another data set and with a lower statistics than in the present paper, are in agreement with the results shown in Table 2.

The main distinctive feature of the $\bar{p}p \to \phi\eta$ channel is the increase in the annihilation frequency for annihilation in gas at low pressure. In terms of the branching ratios it leads to the conclusion that the branching ratio from the spin singlet $^1P_1$ state is 10 times higher than the branching ratio from the spin triplet $^3S_1$ state (see Eqs. (9 - 12)). Just the opposite tendency was observed for the $\bar{p}p \to \phi\pi^0$ channel [5], where the branching ratio from the $^3S_1$ initial state is at least 15 times larger than from the $^1P_1$ one.

The unusual spin dependence of the $\phi\pi^0$ production was explained in [13] under the assumption that the $s\bar{s}$ pairs in the nucleon are polarized, as suggested by the experiments on deep inelastic lepton scattering (for review of experimental results, see [14]). Following this model, the observed strong violation of the OZI rule is only apparent, because it is due to additional production of ϕ by the connected diagrams that are allowed if the nucleon wave function contains a number of $s\bar{s}$ pairs. The model predicts that the ϕ production should be enhanced from the spin

triplet initial states, whereas production of the $\bar{s}s$ pair with total spin $S = 0$ should be enhanced from the spin singlet initial states. Since η meson has a substantial $\bar{s}s$ component, the production of the $\phi\eta$ final state could be regarded as a production of two $\bar{s}s$ pairs, one in the spin triplet state and the other in the spin singlet state. The extension of the polarized intrinsic strangeness model for such case is not straightforward. We note also that the same strong enhancement of η production from the initial spin singlet state was observed in $pp \to pp\eta$ and $pn \to pn\eta$ reactions [15]. An attempt to interpret this effect in the polarized nucleon strangeness model was done in [16].

In some models opulent production of the ϕ meson in $\bar{p}p$ annihilation at rest is assumed to be due to the rescattering diagrams with K^*K or $\rho\rho$ in the intermediate state (see [17], [18]) and references therein). Calculations of the triangle diagram with K^*K intermediate states [18] give for the branching ratio of the $\phi\eta$ from ${}^3S_1$ initial state $B.R.({}^3S_1 \to \phi\eta) = (0.3 \pm 0.1) \cdot 10^{-4}$, a value not far from our experimental results (9-12). However, these approaches could predict neither the observed spin dependence of the $\phi\pi^0$ final state nor the spin dependence of the $\phi\eta$ channel.

An interesting possibility considered in [19] is that the final state interaction (FSI) of two kaons could enhance the ϕ production. Indeed, for annihilation at rest the space volume of $KK\eta$ final state is quite limited, two kaons are created with low relative momenta and could, in principle, fuse into ϕ due to the FSI. However this model does not explain why the FSI effects are stronger for annihilation from the P-wave than from the S-wave.

An attempt to calculate the ϕ yields in $\bar{p}p$ annihilation at rest in a non-relativistic quark model with the $\bar{s}s$ admixture in the nucleon wave function was done in [20]. It was assumed that the ϕ is produced as a "shake-out" of the nucleon $\bar{s}s$ component. The calculated branching ratios of the $\phi\eta$ channel are $B.R.({}^3S_1 \to \phi\eta) = (1.4 - 1.8) \cdot 10^{-4}$ and $B.R.({}^1P_1 \to \phi\eta) = (0.15 - 0.2) \cdot 10^{-4}$. Therefore this "shake-out" mechanism predicts a trend which is exactly opposite to that experimentally observed by us.

The increasing of the $\phi\eta$ yield with the decreasing of the target density arises the question of the corresponding behaviour of the $\bar{p}p \to \omega\eta$ channel. This yield was measured only for the annihilation in liquid [3] and it is quite high: $\mathcal{F}(\omega\eta) = (1.51 \pm 0.12) \cdot 10^{-2}$. If the arguments of the polarised strangeness model are valid for the η production, then the yield of the $Y(\omega\eta)$ final state from the ${}^1P_1$ state should be higher than from the ${}^3S_1$ final state. It would be interesting to verify this prediction experimentally since we have demonstrated that the branching ratio of the $\phi\eta$ channel significantly increases for the P-wave annihilation. If the ratio between the $\phi\eta$ and $\omega\eta$ channels does not change with the hydrogen target density, the apparent OZI violation will be absent for annihilation in low pressure gas as it is for annihilation in liquid.

In conclusion, the $\bar{p}p$ annihilation at rest into $\phi\eta$ final state was measured at three different target densities: liquid, NTP, 5 mbar. The yield of this reaction for the liquid hydrogen target is smaller than for the low pressure gas target. The branching ratios of $\phi\eta$ channel were calculated on the basis of simultaneous analysis of the three data samples. The branching ratio for annihilation into $\phi\eta$ from the ${}^3S_1$ protonium state turns out to be about ten times smaller as compared to the one from the ${}^1P_1$ state. An opposite trend was observed [5] for the $\phi\pi$ final state.

We would like to thank the technical staff of the LEAR machine group for their support during the runs. We are grateful to J.Ellis, D.Kharzeev and V.Markushin for the stimulating discussions.

References

[1] S. Okubo, Phys. Lett. **B 5** (1963) 165;
G. Zweig, CERN Report **No.8419/TH412** (1964);
I. Iizuka, Prog. Theor. Phys. Suppl. 37 **38** (1966) 21.

[2] M.G. Sapozhnikov, JINR preprint **E15-95-544**, (1995).

[3] C. Amsler et al.,Phys. Lett.. **B 346** (1995) 363.

[4] V.G. Ableev et al., Nucl. Phys. **A 594** (1995) 375.

[5] The OBELIX collaboration. A. Bertin et al., *Proceedings HADRON'95 Conference*, (Manchester, 1995) 337.

[6] C. Amsler et al. Phys. Lett. **B 319** (1993) 373.

[7] C.J. Batty, Nucl. Phys. **A 601** (1996) 425.

[8] A. Adamo et al., Sov. J. Nucl. Phys. **55** (1992) 1732.

[9] Spanier, S. Workshop on *The Strange Structure of the Nucleon*, CERN, 1997 (unpublished).

[10] J. Reifenrother, *Proceedings LEAP-90 Conference*, (Stockholm, 1990).

[11] A. Zoccoli, Proceedings of the HADRON Conference, Brookhaven (1997), in press.

[12] J. Reifenrother et al., Phys. Lett. **B 267** (1991) 299.

[13] J. Ellis et al., Phys. Lett. **B 353** (1995) 319.

[14] The SMC Collaboration, B. Adeva et al., *Phys.Lett.* **B412** 414 (1997).

[15] E. Chiavassa et al., Phys. Lett. **B 337** (1994) 192.

[16] M. Rekalo, J. Arvieux, E. Tomasi-Gustafsson, Phys. Rev. **C 55** (1997) 2630.

[17] O.E. Gortchakov, M.P.Locher, V.E.Markushin, S. von Rotz, Z.Phys. **A 353** (1996) 447.

[18] D.Buzatu, F.M.Lev , Phys. Lett. **B 329** (1994) 143.

[19] V.E.Markushin, M.P.Locher, Eur.Phys. J. A1 (1998) 91.

[20] T.Gutsche, A.Faessler, G.D.Yen, S.N.Yang, Nucl. Phys. **B (Proc.Suppl.) 56A** (1997) 311.